International Journal of GEOMATE, July 2019, Vol.17, Issue 59, pp.90 - 97
Geotec., Const. Mat. & Env., DOI: https://doi.org/10.21660/2019.59.8270
ISSN: 2186-2982 (Print), 2186-2990 (Online), Japan

EVALUATION OF DRAINAGE PROCESS IN POROUS MEDIA BY INVADED PERCOLATION PROBABILITY

*Junichiro Takeuchi[1] and Masayuki Fujihara[1]

[1]Graduate School of Agriculture, Kyoto University, Japan

*Corresponding Author, Received: 25 Oct. 2018, Revised: 30 Dec. 2018, Accepted: 23 Jan. 2019

ABSTRACT: Invasion processes, such as the imbibition and drainage processes, through porous media could be modeled using the invasion percolation model in a pore-network that is extracted from actual or virtual packed grains. It is well known that water retention properties depend on pore structures such as pore shape, pore-size distribution, and pore-connectivity. However, in our previous work, it is confirmed that there is a spatial structure even in a porous medium packed with single-size grains, and that if the spatial structure of the pores is not disturbed, different water retention curves obtained from different pore-size distributions for the imbibition process can be unified into a single curve using the invaded percolation probability (IPP). This is the proposed evaluation method based on the percolation probability (PP). In this study, the drainage process is evaluated using water retention curves and the IPP through numerical experiments. The results show that the different water retention curves were unified into a certain curve based on the PP when the IPP based on pore body and pore throat was employed. Using this evaluation method, we can obtain additional information regarding the proportion of potentially invadable and actually invaded pores and the degree of their spread in the porous media. Hence, it is concluded that this method could be a very useful tool to grasp the state of porous media.

Keywords: Water retention property, Pore-network, Invasion percolation, Percolation probability

1. INTRODUCTION

The displacement of immiscible fluids, such as air and water, in porous media, represented by the drainage and imbibition processes, is quite important for many disciplines including the industrial and agricultural fields. To pursue its underlying principle could lead to a better understanding of the mechanism and more effective usage of porous materials.

It is well-known that the water retention property of soils is variable depending on soil type, and that the variability is caused by pore properties, such as size distribution, geometry, the wettability of grain surface, and connectivity to other pores [1]. However, different water retention curves could be unified into a single curve or several curves if the properties are re-evaluated from a viewpoint of the percolation theory [2]. It was presented that the imbibition process of porous media with various pore-size distributions, which show different water retention curves, can be unified into a single curve if it is evaluated by a method called invaded percolation probability (IPP), while the drainage process shows a certain level of variability [3,4]. Invaded percolation is based on the percolation probability (PP), which is used for evaluating the degree of connectivity of a network. It has also been presented that randomly packed pores of single-size spherical grains have a positive spatial autocorrelation of approximately 0.19 score in the global Moran and that the pores of virtual porous media randomly generated following a certain probability density distribution have no spatial autocorrelation [5]. Furthermore, it has been revealed that the imbibition process is strongly affected by spatial autocorrelation [4]. In this study, the dependency of spatial autocorrelation and the cause of the variability in the IPP of the drainage process are investigated through numerical experiments.

2. METHOD

2.1 Pore-network Model

From a virtual porous media constructed by the random packing of single-size spherical grains using the discrete element method, a pore-network model is extracted with the modified Delaunay tessellation method proposed by Al-Raoush et al. (2003) [6]. A pore-network model comprises pore bodies (PBs), which are relatively large pores formed by four or more grains, and pore throats (PTs), which are relatively small pores that connect two PBs [7]. Through the extraction process, the coordinate, size, and connectedness to the surrounding pores of each pore are obtained. The PBs are represented as a sphere, the sizes of which equal the maximum inscribed sphere in each gap formed grains. The PTs are represented as a tube, the length of which is that between the two PBs that

the PT connects, and the size is the maximum inscribed circle in a gap formed by grains.

If the PBs and PTs are regarded as sites and bonds, respectively, which are the terms in the percolation theory, the extracted pore-network model can be presumed to be a network, literally. Each element (site or bond) has a state of 'open' or 'closed'. When an element is 'open', the element can convey something (the objective depends on the target system) to the neighbor elements. Then, the network can convey it holistically if it has enough open elements. Thus, the connectivity of a network is quite an important index.

Distributions of the coordinate number and the PP were analyzed to determine the connectivity of the pore-network as a network. The coordinate number is the number of sites/bonds that a site/bond connects to, and the PP is one with which a site/bond belongs to the infinite 'open' cluster in a case of an infinite network when a certain probability for 'open' is given to a network. In the case of a finite network (the presented case is also finite), the PP is calculated as the proportion of the size of the maximum 'open' cluster to the size of the network.

In this pore-network, each pore has a set of two components for a state. One refers to the invadability of the objective pore, while the other refers to the occupied fluid in the pore. The former takes one state from {invadable, uninvadable}, and the latter takes one state from {invaded, not-invaded}. In the case of the drainage process, the invadability index I is defined from the capillary pressure p_{C} and the local air-entry pressure p_{AE} as follows:

$$I = p_{\mathrm{C}} - p_{\mathrm{AE}} \tag{1}$$

with

$$p_{\mathrm{C}} = p_{\mathrm{air}} - p_{\mathrm{water}} \tag{2}$$

$$p_{\mathrm{AE}} = P\sigma\cos\theta / A \tag{3}$$

$$p_{\mathrm{water}} = p_{\mathrm{btm}} - \Delta z \tag{4}$$

where p_{air} and p_{water} are the air- and water-pressures in the vicinity of an air-water interface, respectively; p_{air} is constant here. A and P are the cross-sectional area and circumference of the inscribed circle in a pore, respectively, σ and θ are the surface tension of water and the receding contact angle, respectively, p_{btm} is the water pressure imposed on the pore-network bottom, and Δz is the difference in height between the bottom and the objective pore. If $I > 0$, the pore is invadable. Namely, air can invade the pore. If $I \le 0$ the pore is uninvadable.

When a certain pressure condition for the air and water is given, the former state of all pores is determined, assuming that each pore is facing an air-water interface that satisfies the continuity rule, as described below. If the proportion of the invadable pores is large enough, fluid begins invading continuously in the invasion percolation manner. The threshold of the proportion, referred to as the critical percolation threshold, is quite important for soil science and corresponds to the air and water entry pressures in the drainage and imbibition processes, respectively. From the critical percolation threshold, we can determine how many pores must be invadable to begin imbibition or drainage.

2.2 Invasion Percolation

A displacement process of immiscible fluids in a pore-network is modeled by the invasion percolation [8]. The invasion percolation is a temporally and spatially discretized model of a progressive process whereby one fluid invades the invadable pores occupied by the other fluid. The following settings for the drainage process are given to a pore-network. The top and bottom faces of the pore-network are connected to outside air and water reservoirs, respectively, and the air and water can inflow and outflow freely, but cannot pass through the four side faces.

The procedure of the invasion percolation for a drainage process is described below [9,10].

1. As an initial state, all or part of the pores are occupied by water, and a certain pressure is imposed on the pore-network bottom.
2. All water-filled pores facing the air-filled pores, satisfying the continuity rule, are sorted in descending order of invadability.
3. The top N^{IP} pores are invaded by air (i.e., water in the pore is drained) simultaneously, where N^{IP} is the number of pores invaded in one-time step.
4. Processes 2 and 3 are iterated until no pores change their state, and the saturation and IPP are calculated.
5. The pressure imposed on the bottom is changed, and the process returns to step 1 or 2.

To move an air-water interface, the continuity rule must be satisfied. Namely, both the air and water must connect to their outside reservoir through pores filled with the same kind fluid.

2.3 Invaded Percolation Probability (IPP)

After reaching the steady state in each pressure condition, the IPP and the saturation are calculated. While the water retention curve (WRC) shows the relationship between the pressure head (matric potential) and saturation (water content), the IPP represents the relationship between the proportion of potentially invadable pores and that of actually invaded pores.

In the case of a normal network, the PP is calculated based on sites or bonds (PTs or PBs in a pore-network). As described above, both PBs and PTs play an important role in the invasion

percolation of a pore-network. Hence, in addition to the PB-based and PT-based (invaded) PPs, the PB-and-PT-based (invaded) PPs are proposed in this study.

3. NUMERICAL EXPERIMENTS

In this study, the numerical experiments of five cases were conducted by changing the degree of overlap of the pore-size distributions between the PBs and PTs, the spatial autocorrelation of pores, and/or the shape of pore-size distributions. The numerical experiments have three major objectives. First is the applicability of the IPP, and which IPP is suitable for evaluating the drainage process among the PB-based, PT-based, and PB-and-PT-based IPPs. Second is the effect of the spatial autocorrelation of the pores. Even a porous medium of randomly packed spherical grains with uniform size has spatial autocorrelation, although the degree is low (approximately 0.19 in the global Moran), and has statistical significance [5]. As a standard case, pore-size distributions are shifted without altering the pore-arrangement and the overlap between the PB and PT (Case 1). To eliminate the spatial autocorrelation of the pores, pore-arrangement is randomly shuffled without changing the network topology (Case 3 and Case 4). Third is the effect on the IPP of the overlap of pore-size distributions between the PB and PT. The PT distribution is shifted without changing shape, while the PB distribution is fixed (Case 2 and Case 4). Furthermore, as an ideal case, a uniform distribution is employed for the pore-size distribution, which has no spatial autocorrelation (Case 5).

4. RESULTS AND DISCUSSION

4.1 Pore-network

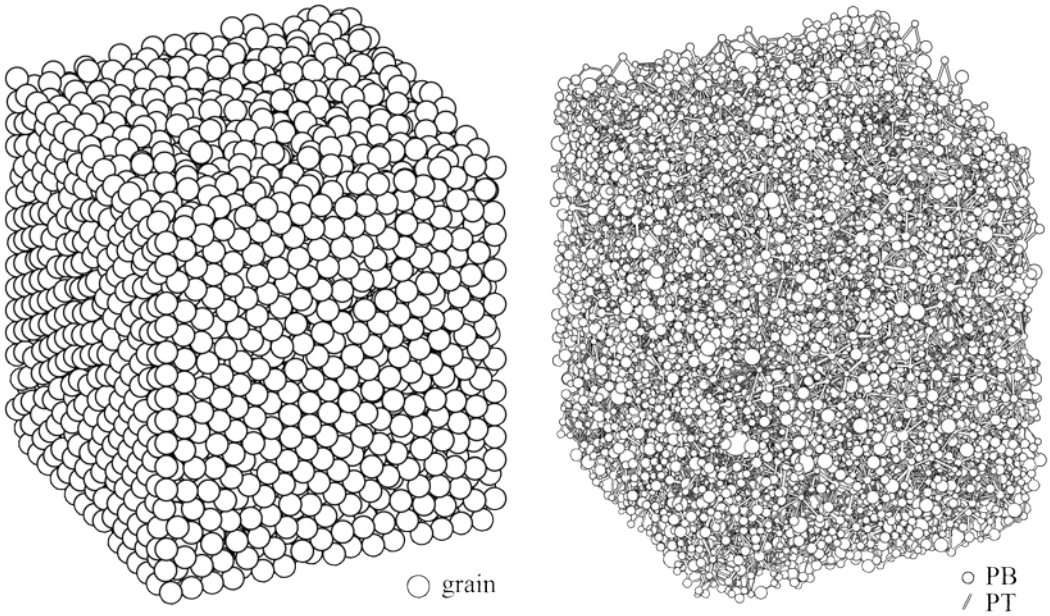

(a) Randomly packed grains (b) Extracted pore-network

Fig. 1 Virtual porous medium

About 5800 spherical grains, with diameters of 0.2 mm, are randomly packed in a 32.8 mm^3

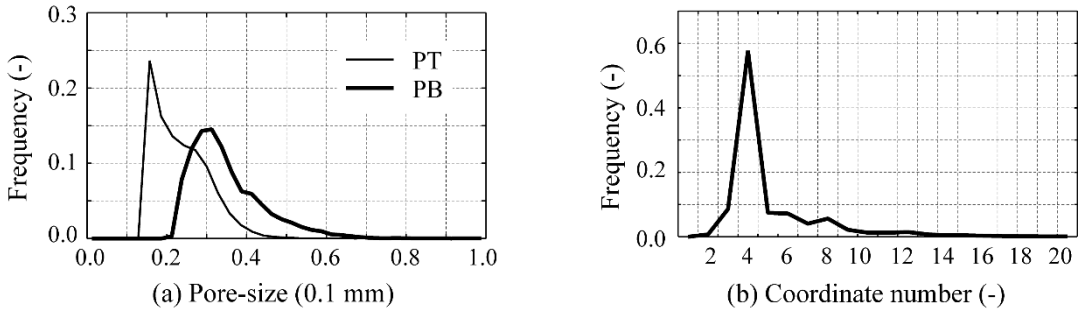

(a) Pore-size (0.1 mm) (b) Coordinate number (-)

Fig. 2 Pore-size and coordinate number

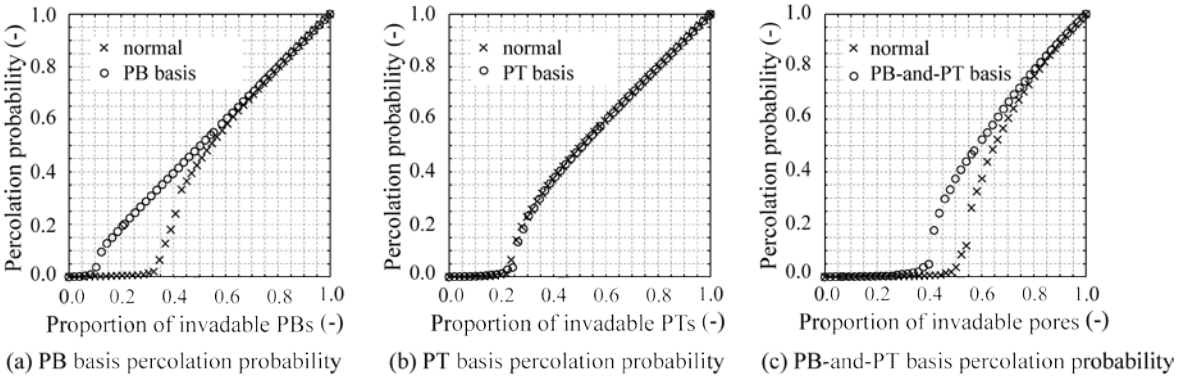

(a) PB basis percolation probability (b) PT basis percolation probability (c) PB-and-PT basis percolation probability

Fig. 3 Percolation probability of pore-network

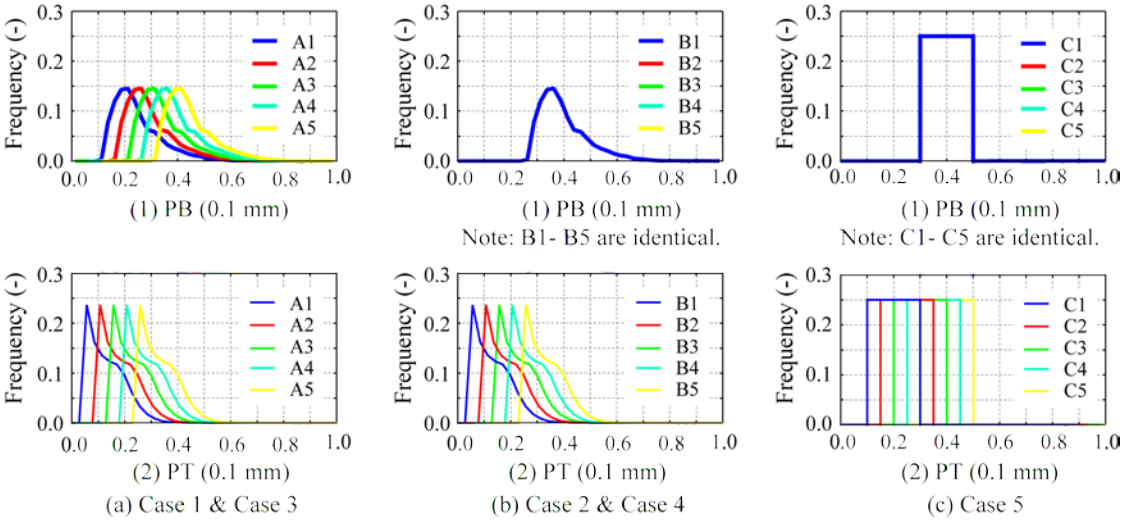

(a) Case 1 & Case 3 (b) Case 2 & Case 4 (c) Case 5

Fig. 4 Pore-size didstributions for numerical experiments

container using the discrete element method (Fig. 1 (a)), and a pore-network is extracted from the virtual porous media (Fig. 1 (b)). The pore-network comprises 13,804 PBs and 35,233 PTs, and the distributions of the pore-size and coordinate number are shown in Fig. 2. The size of the porous medium is sufficiently large compared with the standard proposed by Reeves and Celia (1996) [11] and it was confirmed that similar pore-size and coordinate number distributions were obtained from different grain-packing in the cubic container [4].

4.2 Percolation probability (PP)

The three types of PP, namely, PB-based, PT-based, and PB-and-PT-based, are shown in Fig. 3. In each PP, the pore-size-basis is shown in addition to the normal PP. The normal PP is obtained by giving the PBs and/or PTs a random number within the range of 0 to 1 with a uniform distribution (but the range and the distribution is arbitrary to evaluate the PP generally) to evaluate the connectivity as a pure network. The pore-size-basis is obtained by giving the invadability I, which reflects the spatial autocorrelation of the porous media, instead of the random number.

In Fig. 3 (a), where the connectivity of the PBs is considered, the PB-based PP rises at 0.1 while the normal PP is at 0.35, which implies that PBs have spatial unevenness in the arrangement. It is considered that large pores connect each other and form paths through the medium because a sub-network, that spreads from one end to the other, begins to form when only 10% of the PBs are invadable, although more than 30% or more invadable pores are needed to form a sub-network that spreads in the case of a pure network.

Figure 3 (b) shows that both the normal and PT-based PPs are similar in shape and arise at about 0.2, implying that the PTs have no spatial autocorrelation, like PBs. The PTs have a lower rising point compared with that of the normal PP in the PB-based (i.e., 0.35), demonstrating the ease of the connection of PTs, as PTs have more neighboring (connecting) PTs than PBs.

Figure 3 (c) shows the PPs when both the PB and PT are taken into consideration. The normal corresponds to the C5 distributions in Fig. 4 (c). As revealed in the following subsection, the size relation of the PBs and PTs plays a critical role in

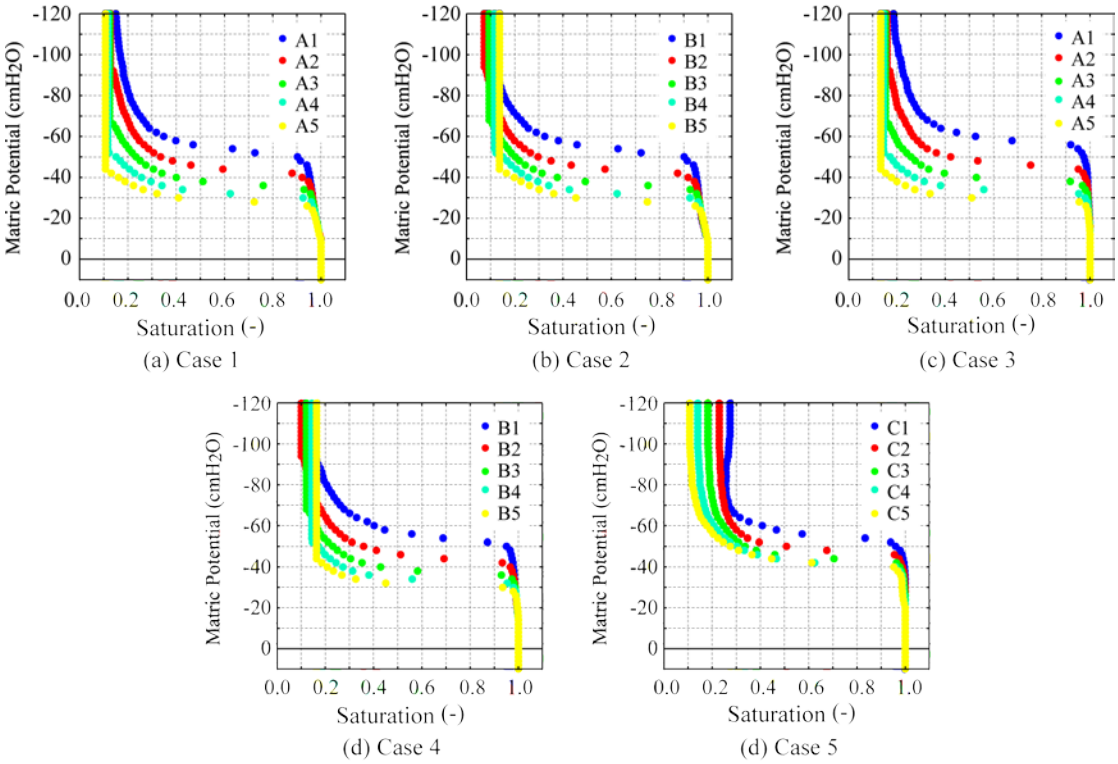

Fig. 5 Water retention curves

forming the PP and IPP. The reason for the lower rising point in the PB-and-PT-based PP is considered to be the effect of the ease of connectivity of the large PBs shown in Fig. 3 (a).

4.3 Water Retention Property

The pore-size distributions used in the numerical experiments are shown in Fig. 4. The A3 distributions in Figs. 4 (a-1) and (a-2) are the originals obtained from the extracted pore-network in Fig. 2 (a). The other distribution set for the PB and PT in Fig. 4 (a) is made by shifting the A3 distributions along the same distance so as not to change the original size relation of the PBs and PTs. These distributions are used for Cases 1 and 3. In Fig. 4 (b), for Cases 2 and 4, the PB distributions are fixed, and only the PT distributions are shifted. The PB distributions correspond to the A4 distribution in Fig. 4 (a-1). For Case 5, the uniform distributions are used, and only the PT distributions are shifted (Fig. 4 (c)) in the same way with Case 2 and Case 4.

The WRCs obtained from the conducted numerical experiments in the five cases are shown in Fig. 5. As expected, the WRCs vary depending on the pore-size distributions. For example, when smaller PTs are used (namely, A1–2, B1–2, and C1–2), the air-entry pressure becomes high.

4.4 PP

The PP of each case is shown in Fig. 6. The PB- and PT-based PPs are omitted here as they are completely identical with those in Fig. 3 (a) or (b). Firstly, the PPs in Case 5 are discussed. Case 5 has uniform distributions with various overlaps between the PB and PT, and the pores do not have spatial autocorrelation. As mentioned above, C5 corresponds to a pure network (Fig. 3 (c)). Figure 6 (e) shows that the rising point moves left as the degree of overlap decreases and that the movement almost peaks when the overlap becomes 50% (Case 3). This indicates that the PP of normal porous media, which have the structure in which more than half the PBs are larger than the PTs and without spatial autocorrelation, becomes the same curve fir C1–C3. Cases 3 and 4, with no spatial autocorrelation, obey this principle. The PPs of all distributions in Case 3 and B1–B4 in Case 4 correspond to the most left PP in Case 5. When the overlap between the PBs and PTs surpasses a certain limit, 50% here, which is the case of B5 in Case 4, the rising point moves left, like C4 in Case 5.

The pores in Case 1 and Case 2 have spatial autocorrelation. All distributions in Case 1 and B4 in Case 2 correspond to the PP of the PB-and-PT-based PP in Fig. 3 (c), because these have the same size relation between PBs and PTs. Unlike the cases without spatial autocorrelation (Case 3–Case 5), Case 2 shows that the rising point of the PP moves left as the degree of overlap between the PBs and PTs increases, which is opposite to Case 5. However, the degree of overlap is considered to be

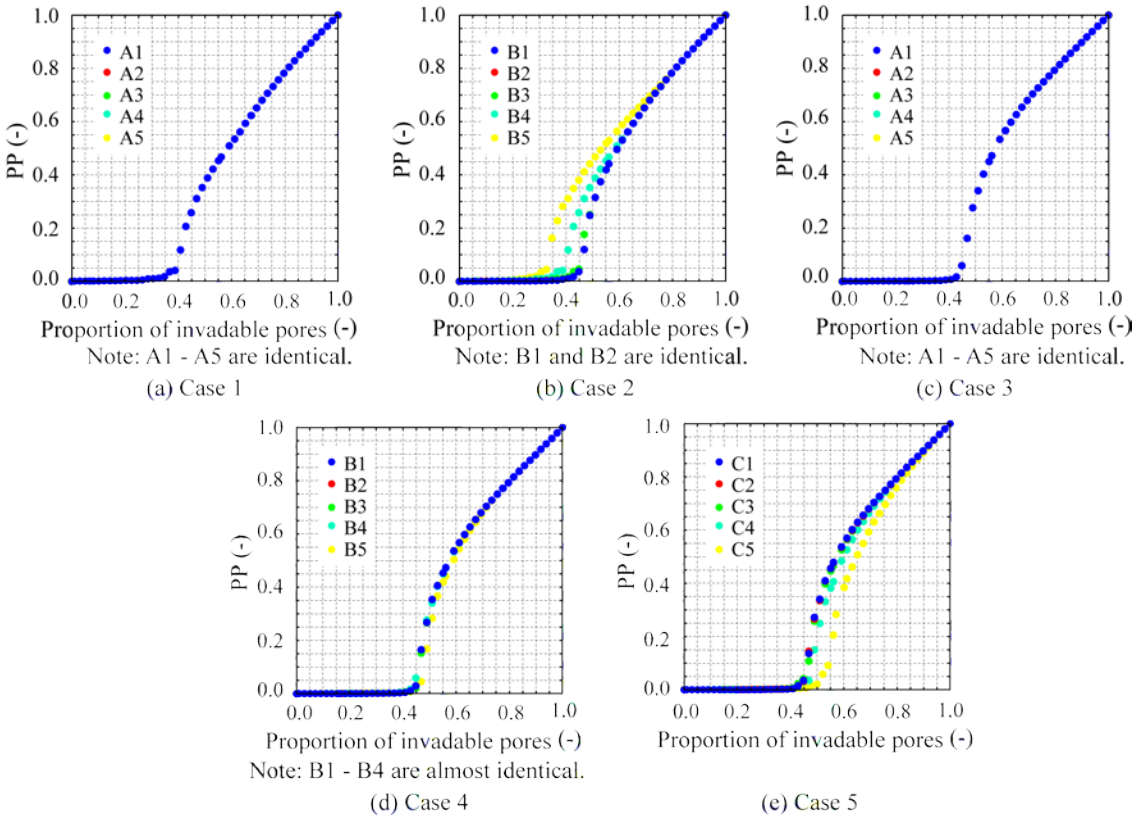

Fig. 6 PB-and-PT basis percolation probability in all cases

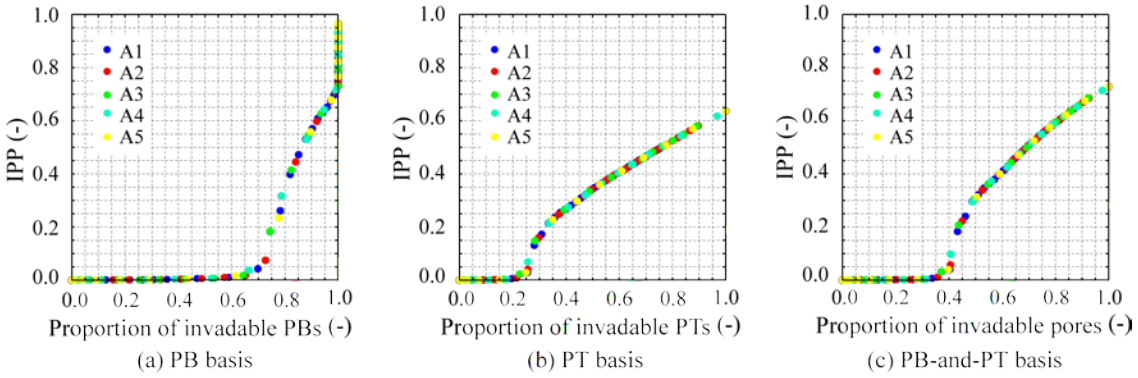

Fig. 7 Invaded percolation probability in Case 1

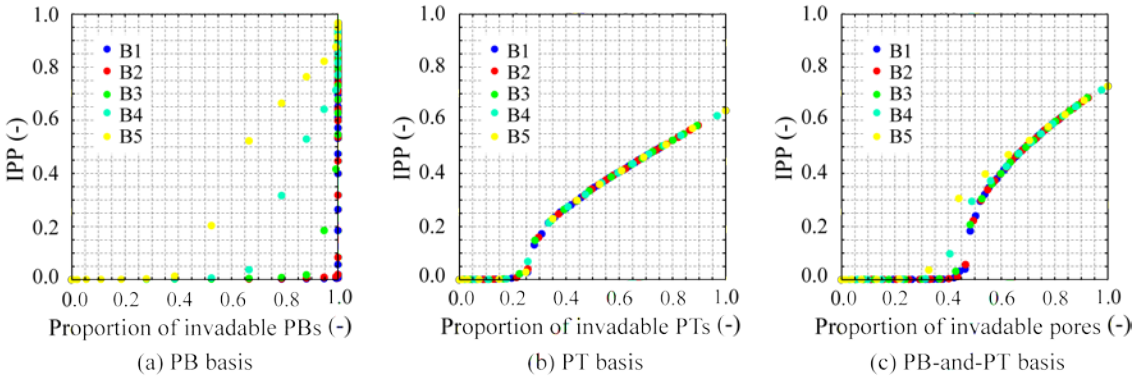

Fig. 8 Invaded percolation probability in Case 2

less than 50% from Case 4; hence, it is estimated that the influence of the overlap is not so large and that the movement of the rising point in Case 2 is mainly caused by the size of the PTs.

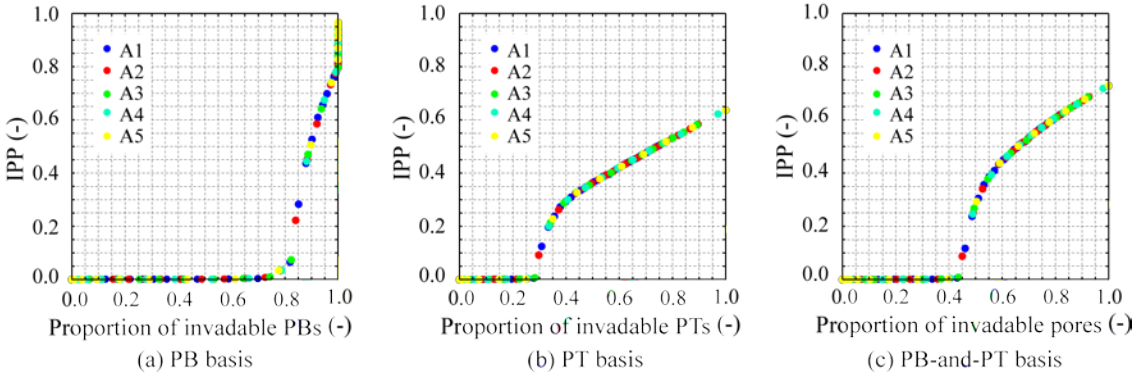

Fig. 9 Invaded percolation probability in Case 3

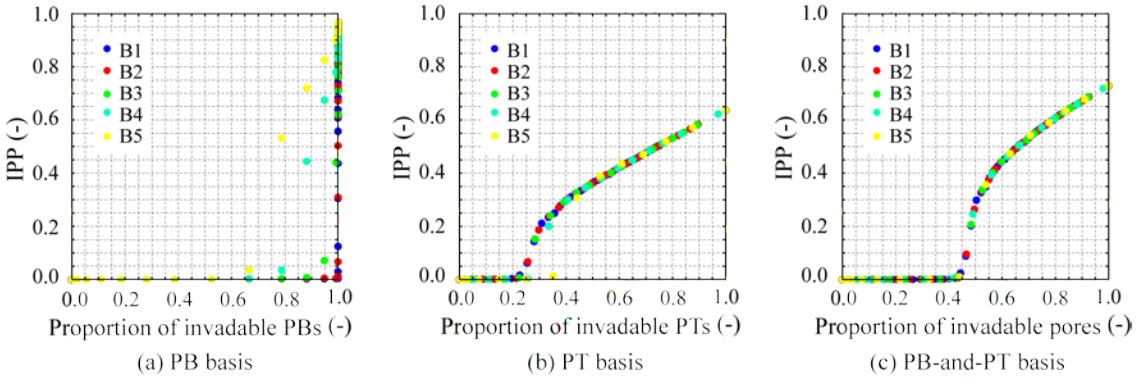

Fig. 10 Invaded percolation probability in Case 4

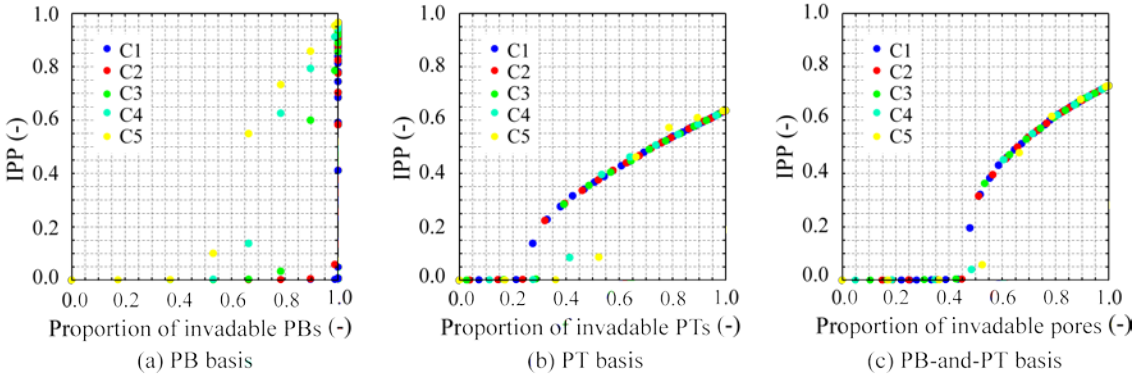

Fig. 11 Invaded percolation probability in Case 5

4.5 IPP

The obtained PB-based, PT-based, and PB-and-PT-based IPPs of all cases are shown in Figs. 7 through 11. Here, which IPP basis should be employed is predominantly discussed to evaluate the drainage process. In the case of the imbibition process, PB-based IPP was selected because water invasion into pores is ruled mainly by PBs, which are larger than PTs [4]. The selected IPP is such that it should obey its PP well, based on the obtained knowledge about PP.

Firstly, the PB-based IPPs in Figs. 7 through 11 (a) do not obey the PB-based PPs in Fig. 3 (a) absolutely, and, hence, the PB-based IPP is excluded.

Secondly, PT-based IPPs in Figs. 7 through 11 (b) obey their PPs well except for B4 and B5 in Case 4 and C3–5 in Case 5. The common factors of these five cases are the relatively large degree of overlap between the PBs and PTs, and no spatial autocorrelation. Moreover, the rising point of the IPP in Case 3 (Fig. 9 (b)) is slightly larger than those in Case 1 and Case 2. Hence, it is considered that the PT-based IPP is applicable, excluding such situations.

Thirdly, the PB-and-PT-based IPPs in Figs. 7 through 11 (c) obey each PP very well, and the changes of the rising points depending on the degree of overlap are also produced well in the IPPs. Hence, the PB-and-PT-based IPP should be used for evaluating the drainage process. The water retention curves, which are the conventional evaluation method, represent the relationship between the

capillary pressure and saturation (or water content), and both axes are physical quantities. The IPP represents the relationship between the proportion of potentially invadable pores and the proportion of actually invaded pores when a certain pressure is imposed. This means that additional information can be determined regarding how the porous medium may potentially and actually contain water when a certain pressure is given. It is considered that this method will be applicable to real porous media because three-dimensional modeling of the pores is available by X-ray CT analysis [12].

5. CONCLUSIONS

In this study, the usefulness of the IPP, which is an evaluation method based on the PP in the percolation theory, was investigated through numerical experiments with a pore-network. In the numerical experiments, the drainage process was modeled by the invasion percolation. Various pore-size distributions were given to the pore-network, and the water retention curves and IPP were calculated. The obtained results show that the water retention curves vary depending on pore-size distribution. Unlike the imbibition process, only the PB-and-PT-based IPP can reproduce the rising point of its original PP, even with various degrees of overlap between the PBs and PTs. This evaluation method is very useful to grasp the state of a porous medium. When a certain pressure is given, we can determine the proportion of potentially invadable pores and the degree of spread of the invadable sub-network from the PP, and the proportion of actually invaded pores from the IPP.

6. ACKNOWLEDGMENTS

This study was supported by JSPS KAKENHI Grant Number 16K07971.

7. REFERENCES

[1] van Genuchten M. T., A Closed Form Equation for Predicting the Hydraulic Conductivity of Unsaturated Soils, Soil Sci. Soc. Am. J., Vol. 44, 1980, pp.892–898.

[2] Hunt A. and Ewing R., Percolation Theory for Flow in Porous Media, Springer, Heidelberg, 2009, p.319.

[3] Takeuchi J., Tsuji H., and Fujihara M., The Effect of Capillary Radius Distribution on the Hydraulic Properties of Porous Media, Precision Farming and Resource Management, Excel India Publishers, New Delhi, 2016, pp.292–304.

[4] Takeuchi J. and Fujihara M., Evaluation of Imbibition Process in Porous Media by Invaded Percolation Probability, Int. J. GEOMATE, Vol. 14, 2018, pp.1–7.

[5] Takeuchi J. and Fujihara M., Spatial Statistical Analysis of Pores in Single-size Grains Packing, Proceedings of JRCSA 2017 Annual Congress, 2017, pp.18–21 (in Japanese).

[6] Al-Raoush R., Thompson K., and Willson C. S., Comparison of Network Generation Technique for Unconsolidated Porous Media, Soil Sci. Soc. Am. J., Vol. 67, 2003, pp.1687–1700.

[7] Fatt I., The network model of porous media, Trans. AIME, Vol. 207, 1956, pp.144–181.

[8] Wilkinson D. and Willemsen J. F., Invasion Percolation: A New Form of Percolation, J. Phys. A: Math. Gen., Vol. 16, 1983, pp.3365–3376.

[9] Takeuchi J., Sumii W., and Fujihara M., Modeling of Fluid Intrusion into Porous Media with Mixed Wettabilities Using Pore-network", Int. J. GEOMATE, Vol. 10, 2016, pp.1971–1977.

[10] Takeuchi J., Tsuji H., and Fujihara M., Modeling of Permeability of Porous Media with Mixed Wettabilities Based on Noncircular Capillaries, Int. J. GEOMATE, Vol. 12, 2017, pp.1–7.

[11] Reeves P. C. and Celia M. A., A Functional Relationship between Capillary Pressure, Saturation and Interfacial Area as Revealed by a Pore-scale Network Model", Water Resour. Res., Vol. 32, 1996, pp.2345–2358.

[12] Mukunoki T., Miyata Y., Mikami, K., and Shiota E., X-ray CT analysis of pore structure in the sand, Solid Earth, Vol. 7 (3), 2016, pp.929–942.